Metal-directed columnar phase formation in tetrahedral zinc(II) and manganese(II) metallomesogens

Journal Item

Metal-directed columnar phase formation in tetrahedral zinc(II) and manganese(II) metallomesogens†

Francesca Morale,[a] Rachel L. Finn,[a] Simon R. Collinson,[a] Alexander J. Blake,[a] Claire Wilson,[a] Duncan W. Bruce,*[b] Daniel Guillon,[c] Bertrand Donnio*[c] and Martin Schröder*[a]

Received (in Durham, UK) 13th July 2007, Accepted 13th August 2007
First published as an Advance Article on the web 25th September 2007
DOI: 10.1039/b710745e

New, non-discoid M(II) complexes $[MCl_2(L)]$ {M = Mn, Zn; L = 2,6-diformyl-4-methylphenolbis[3′,4′,5′-tris(hexadecyloxy)phenylimine]} have been prepared and shown to exhibit columnar mesophases, the nature of which was found to be metal-dependent. As analysed by DSC and small-angle X-ray diffraction experiments, the complex $[ZnCl_2(L)]$ exhibits a single mesophase with rectangular symmetry (Col_r) between 46 and 145 °C, whereas the Mn(II) analogue $[MnCl_2(L)]$ displays a purely hexagonal mesophase (Col_h) phase between 55 and 285 °C. By combining these results with those obtained from dilatometry, a model for the molecular organisation within the columnar mesophases is proposed. The single-crystal X-ray structure of the related complex $[Zn(NO_3)(L')_2]NO_3 \cdot 3MeOH$ {L′ = 2,6-diformyl-4-methylphenolbis[3′,4′,5′-tris(methoxy)phenylimine]} has been determined and supports the proposed mode of binding of the ligand to the metal *via* only one imine and a phenol.

Introduction

Metal complexes derived from Schiff-base ligands feature amongst the earliest and most widely studied class of metallomesogens.[1] The advantages of incorporating the imine functionality lie in the diverse range of potential structures and their ease of preparation. Consequently, this versatile functionality has produced metallomesogens of thermotropic liquid crystals,[2] surfactants,[3] polycatenar mesogens,[4] polymers,[5] luminescent materials,[6] magnetic materials,[7] ferrocene,[8] chiral complexes[9] and metallohelicates.[10] Schiff-base ligands have found widespread use[11] and are often obtained by the condensation of 2,6-dicarbonyl compounds with primary amines. Of particular relevance here are the acyclic 2,6-phenoldiimines of the 'end-off' type,[12] which are [1 + 2] Schiff-base products (Fig. 1a), and which are readily derivatised given the vast choice of amine starting materials available. These commonly incorporate functional groups (designated as Y in Fig. 1a). Related to this, reaction between monocarbonyl compounds and primary diamines in 2 : 1 stoichiometric ratios yields Schiff-base chelates of the 'side-off' type (Fig. 1b), while macrocyclic products (Fig. 1c) are afforded by [2 + 2] Schiff-base condensation with primary diamines.

Of note here are the Robson-type Schiff-base compounds,[13] where imino derivatisation of the central phenol ring at the two *ortho* positions results in typical 'bent-core' or 'U-shaped' chelate moieties able to bind two metals simultaneously in the adjacent NO-'compartments' (Fig. 2a). The two, six-membered chelate rings formed by the compartmental 2,6-diiminophenol unit upon complexation to two metal ions share the central *O*-donor atom, which acts as an endogeneous bridge in its anionic form. The metal ions can be found either lying in the NON-plane of co-ordination or displaced from it and, in some binuclear species, both situations have been observed simultaneously.[11c] The environments of the bound metal ions can be extremely diverse as co-ordinative unsaturation of the metal encourages the presence of additional donors, often acting as inter-metallic bridges of the exogeneous type. Moreover, these binuclear complexes often also exhibit what has been termed 'co-ordination number asymmetry',[14] where inequivalence at the two central sites is the result of preferential metal-binding by the external ligating groups.

A peculiarity of this NON-ligand motif is that mononuclear species will be formed should the central hydroxyl proton be retained upon complexation (Fig. 2b). In the cases where mononuclear products are observed,[15] the neutral chelate system HL binds one metal *via* one NO-donor set, while the

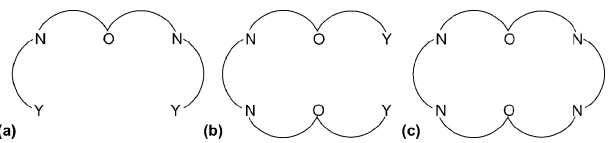

Fig. 1 Phenol-based acyclic and macrocyclic Schiff-base ligands; (a) 'end-off' ligands, (b) 'side-off' ligands and (c) macrocyclic ligands. Adjacent metal-binding compartments (NO/YO) share the central bridging donor atom (O). Y is a functional co-ordinating group.

[a] *School of Chemistry, University of Nottingham, University Park, Nottingham, UK NG7 2RD. E-mail: M.Schroder@Nottingham.ac.uk; Fax: (+44) 115 9513563*
[b] *Department of Chemistry, University of York, Heslington, York, UK YO10 5DD. E-mail: db519@york.ac.uk; Fax: (+44) 1904 432516*
[c] *Institut de Physique et Chimie des Matériaux de Strasbourg (IPCMS), UMR 7504 (CNRS-ULP), 23 rue du Loess, BP 43, F-67034 Strasbourg Cedex 2, France. E-mail: bdonnio@ipcms.u-strasbg.fr; Fax: (+33) 388 10 72 46*

† Electronic supplementary information (ESI) available: Schematic representation of the various parameters defining the columnar packing. See DOI: 10.1039/b710745e

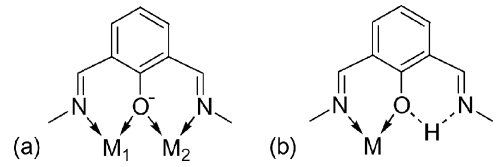

Fig. 2 (a) A 2,6-functionalised phenol-based diimine displays a 'bent-core' upon co-ordination to two metal ions. The planar NON-donor set features distinctive chelation modes, forming two adjacent, six-membered ring compartments with a communal endogenous O-bridge in binuclear compounds. (b) The mononucleating behaviour of neutral 2,6-di-iminophenol chelates (HL) with associated intramolecular H-bonding taking place in one of the NO-cavities.

non-metal binding NO-donor set has an intramolecular hydrogen bond between the phenolate oxygen and the other protonated imine nitrogen.

With the aim of developing novel mesomorphic materials, the present work focuses on a phenol-based 2,6-diimine ligand (L) of the 'end-off' type, bearing six alkoxy chains (R = $C_{16}H_{33}$) attached to the two lateral phenyl substituents. The first-row transition metal ions chosen for this investigation were Mn(II) (d^5) and Zn(II) (d^{10}), and it was anticipated that such angular complexes with asymmetric occupancy of the phenolic-imine compartments might lead to interesting liquid-crystalline properties *via* assembly and packing of molecules in the mesophase (Fig. 3).[16] Additionally, in our design we targeted mononuclear complexes incorporating intramolecular hydrogen bonding between one imine and the phenol. We have reported previously lanthanide iminophenolate metallomesogens where the metal cation is bound to the phenolic oxygen and the imine nitrogen is protonated.[2e–g] To the best of our knowledge, however, liquid crystals derived from 2,6-diiminophenols have not yet been reported in the literature.

We report herein the synthesis and characterisation of new metallomesogens $[MCl_2(L)]$ {M = Mn, Zn; L = 2,6-diformyl-4-methylphenolbis[3′,4′,5′-tris(hexadecyloxy)phenylimine]}. The mesomorphic behaviour of these complexes was evaluated by a combination of complementary techniques including polarised optical microscopy, differential scanning calorimetry (DSC), small-angle X-ray diffraction and dilatometry. Complexation of the analogous ligand L′ {L′ = 2,6-diformyl-4-methylphenolbis[3′,4′,5′-tris(methoxy)phenylimine]} was also studied as a model species with the aim of producing complexes suitable for study by single crystal X-ray diffraction, and this was achieved for the complex $[Zn(NO_3)(L')_2]NO_3 \cdot 3MeOH$.

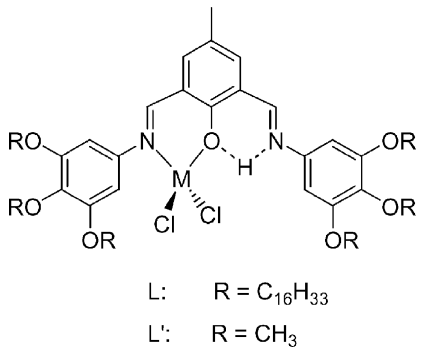

Fig. 3 View of the mononuclear complex of neutral 2,6-diformyl-4-methylphenolbis[3′,4′,5′-tris(hexadecyloxy)phenylimine] (L), adopting a 'U-shape' upon complexation and by virtue of intramolecular H-bonding.

Results and discussion

Synthesis

The complexes $[MCl_2(L)]$ (M = Mn, Zn) were prepared by template [1 + 2] Schiff-base condensation of 2,6-diformyl-4-methylphenol[17] with two molar equivalents of 3,4,5-tris(hexadecyloxy)aniline[18] in the presence of one molar equivalent of MCl_2 (Scheme 1a). The mixture was heated under reflux overnight and then left to stand at room temperature. The final products were isolated in high yield following slow concentration of the reaction mixture; the precipitates thus obtained did not require further purification. The brightly coloured complexes appeared as waxy solids, most probably due to the presence of the long hydrocarbon chains. The free ligands L and L′ were also prepared in order to test their thermal stability and behaviour.

Given the possibility of obtaining chemical species of variable stoichiometric composition, metal chloride salts were favoured in order to generate neutral 1 : 1 metal–ligand complexes of the type $[MCl_2(L)]$ (Fig. 4), intended for comparison with the pyridyl analogues.[16a] It was envisaged that introducing chloride co-ordinating counterions will discourage the formation of cationic 1 : 2 metal–ligand complexes as was found for the product $[Zn(NO_3)(L')_2]^+$ formed by reaction of $Zn(NO_3)_2$ with L′ (Scheme 1b). Furthermore, the low basicity of the chloride ions will help maintain a neutral phenol system and thus avoid the formation of 2 : 1 metal–ligand species. It was also anticipated that compounds of 2 : 2 metal–ligand stoichiometry of type $[M_2(L)_2]^{n+}$, observed only in cases of

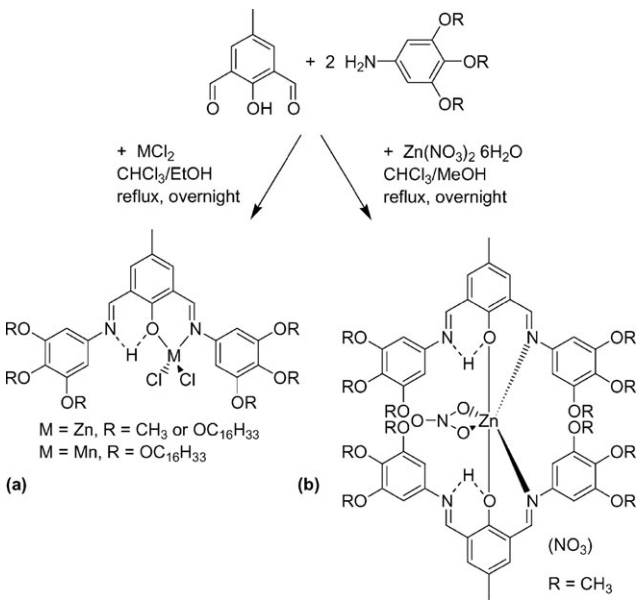

Scheme 1 Scheme for the preparation of the manganese(II) and zinc(II) complexes of 2,6-diformyl-4-methylphenolbis[3′,4′,5′-tris(alkoxy)phenylimine] [R = $C_{16}H_{33}$ (L); R = CH_3 (L′)] *via* a template [1 + 2] Schiff-base condensation.

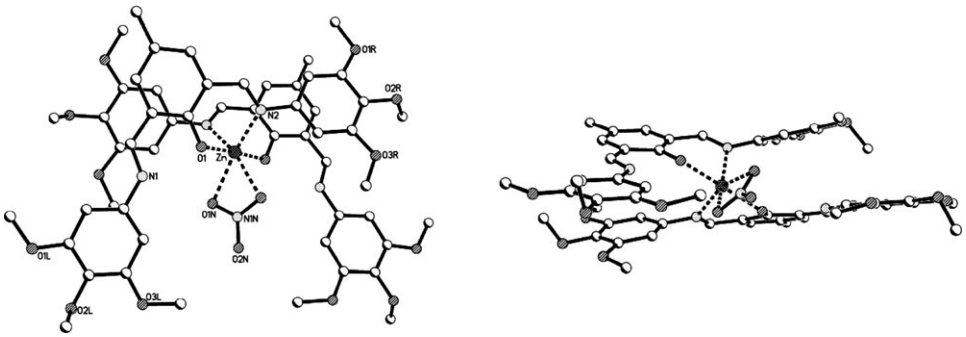

Fig. 4 Left: view of the cation in the molecular structure of $[Zn(NO_3)(L')_2]NO_3 \cdot 3MeOH$. Two ligands bind the Zn ion asymmetrically *via* only one NO-compartment and a nitrate ion completes the distorted octahedral co-ordination environment. The other nitrate anion, solvent molecules and hydrogen atoms have been omitted for clarity. Right: a view of the complex showing the torsion of the lateral phenyl rings minimising steric crowding.

non-bulky imino substituents present on the ligand framework,[19] were unlikely to form due to the presence of the voluminous alkyl chains on L.

Characterisation

The ligands L, L′ and their corresponding complexes were characterised by infrared spectroscopy, mass spectrometry and elemental analysis, with the additional use of ^1H and ^{13}C NMR spectroscopy for the free ligands and the diamagnetic Zn(II) complexes.

The infrared spectra of the products do not contain bands assignable to the amine and carbonyl absorptions associated with the starting aniline and dialdehyde materials, respectively, with the imine stretching vibrations occurring as two bands centred around 1620–47 and 1590 cm^{-1}. In the infrared spectra of the ligands, the higher frequency imine absorption is of weak intensity, whereas for $[MnCl_2(L)]$, $[ZnCl_2(L')]$ and $[Zn(NO_3)(L')_2][NO_3]$, this stretch appears as a band of intensity comparable to the lower frequency imine stretch. Moreover, both signals undergo blue shifts of between 7 and 21 cm^{-1} upon complexation. This is particularly accentuated for the high frequency band, which shifts by between 10 and 21 cm^{-1}. The fact that it is one particular absorption band that is affected predominantly by metal ion complexation, is consistent with the formation of an unsymmetric complex. The high frequency imine stretch is, therefore, assigned to the metal-bound imine.

^1H NMR spectroscopy confirms the unsymmetrical nature of $[ZnCl_2(L)]$ by revealing doubling of many signals found in the spectrum of the ligand L. Thus, the metal-free ligand shows two equivalent imine protons as a singlet at $\delta = 8.8$, while the aromatic region shows two other singlets arising from the *meta*-protons of the phenol ring and from the *ortho*-protons of the lateral phenyl substituents (around δ 7.3 and 6.5, respectively). In the aliphatic region, the first methylene groups of the alkoxy chains give rise to overlapping triplets at around δ 4.0. On complexation, doubling of the above resonance in the ^1H NMR spectrum is particularly evident for the imine and aromatic protons, and six singlets from these groups can now be identified in the region δ 9.4 to 6.6 for $[ZnCl_2(L)]$. Likewise, resonances in the ^{13}C NMR spectrum for the imine and aromatic regions recorded for metal-free L are doubled for $[ZnCl_2(L)]$ and are consistent with the complex losing the symmetry of the ligand, L. All assignments by ^{13}C NMR spectroscopy were made using carbon–hydrogen shift correlation experiments. Microanalytical data and mass spectrometry are also in agreement with a formulation of the products as 1 : 1 metal–ligand species with two chloride ligands completing the metal co-ordination environment. Tetrahedral geometries are assigned to the complexes $[MnCl_2(L)]$ and $[ZnCl_2(L)]$ by comparison with related literature examples.[20] The binding mode of the ligand is further supported by the crystal and molecular structure of $[Zn(NO_3)(L')_2]NO_3$ (L′ = 2,6-diformyl-4-methylphenol-bis[3′,4′,5′-tris(methoxy)phenylimine]).

Single-crystal X-ray structure of $[Zn(NO_3)(L')_2]NO_3$ {L′ = 2,6-diformyl-4-methylphenolbis[3′,4′,5′-tris(methoxy)phenylimine]}

The complexes $[ZnCl_2(L')]$ and $[Zn(NO_3)(L')_2]NO_3$ were prepared according to the same procedure as that above for the long-chain homologous complexes. Orange needles of the $[ZnCl_2(L')]$ were formed by allowing the ligand in CH_2Cl_2 and $ZnCl_2$ in MeCN to diffuse and react together slowly over a number of weeks. Unfortunately, due to the poor quality of the crystals, a full structure determination could not be achieved. However, the structure of a closely-related mononuclear $ZnCl_2$ complex of a diiminophenol ligand has recently been reported,[20a] and this confirms the nature of our complexes prepared herein. The reported complex shows one Zn(II) ion co-ordinated in a tetrahedral geometry to a $NOCl_2$ donor set, the second imine nitrogen donor being protonated and involved in hydrogen bonding with the phenolate oxygen.

Single red cube-like crystals of $[Zn(NO_3)(L')_2]NO_3 \cdot 3MeOH$ were obtained *via* vapour diffusion of diethyl ether into the original reaction solution in $CHCl_3$–MeOH. The structure of the complex shows the Zn atom lying on a 2-fold rotation axis with the asymmetric unit consisting of 0.5 Zn, one ligand L′, half a bound nitrate (where the second ligand and remainder of the Zn and nitrate are symmetry-generated) and a half-occupied unbound nitrate (a symmetry-generated equivalent is adjacent to this site) and 1.5 MeOH.

Table 1 Selected crystallographic data for $[Zn(NO_3)(L')_2]NO_3 \cdot 3MeOH$

Chemical formula	$C_{57}H_{72}N_6O_{23}Zn$
Formula weight/g mol^{-1}	1274.58
Crystal system	Monoclinic
Space group	$C2/c$
Crystal colour	Dark red
Crystal dimensions/mm	0.35 × 0.32 × 0.30
a/Å	17.358(2)
b/Å	14.1481(14)
c/Å	24.213(2)
α/°	90.00
β/°	92.636(2)
γ/°	90.00
V/Å^3	5940.0(10)
T/K	150(2)
Z	4
D_c/g cm^{-3}	1.425

Selected crystallographic data are provided in Table 1 and selected bond angles and bond lengths in Table 2.‡

The Zn(II) ion in $[Zn(NO_3)(L')_2]^+$ is bound by a bidentate nitrato group and the NO-donor sets from two bidentate ligand molecules to give a distorted octahedral geometry (Fig. 4, left). The remaining imine N-centre of the ligand is protonated and forms an intramolecular hydrogen bond (O···H 1.88 Å) to the phenolate oxygen,[21] supporting a binding mode for the ligand L′ similar to that suggested[20a] for the complex $[ZnCl_2(L')]$. The two phenolate oxygen groups are in mutually *trans* positions with a ligand bite angle of 85.8°; the ligand is twisted at the bound imine N-centres with torsion angles of −1.7° and 14.9° for C1–C2–C8–N1 and C1–C6–C9–N2, respectively. The lateral trimethoxyphenyl rings attached to the free imininium N-centre are almost coplanar with the central phenolate ring (interplanar angle of 4.5°), whereas the trimethoxyphenyl ring of the bound imine nitrogen is at an angle of 25.9° to the phenolate ring and 21.6° to the other trimethoxyphenyl ring. However, it is much closer to coplanarity to the phenolate ring of the other ligand L′, with an angle of 10.6° between these planes (Fig. 4, right).

Mesomorphic behaviour

The metal-free ligand with six hexadecyloxy chains (L) was found to show no mesomorphism, as anticipated given its expected bent molecular structure and small molecular anisotropy. However, on co-ordination to MCl_2 fragments mesomorphism was induced, reflecting conformational rigidification of the ligand on complexation. Significantly, the mesophases exhibited by these materials exist over large temperature ranges, illustrating mesophase induction and a stabilisation effect upon complexation.[1] Moreover, the choice of the metal ion seems to affect the observed mesomorphism quite radically.

The complexes $[MCl_2(L)]$ were investigated by polarised optical microscopy, but this technique was not sufficient to allow the phases to be assigned unequivocally. Thus, the materials were further studied by X-ray diffraction (*vide infra*). DSC experiments confirmed the presence of phase transitions,

‡ CCDC reference number 656905. For crystallographic data in CIF format see DOI: 10.1039/b710745e

Table 2 Selected bond distances and angles for $[Zn(NO_3)(L')_2]NO_3 \cdot 3MeOH$

Atoms	Distance/Å	Atoms	Angle/°
Zn–O1	2.0221(19)	O1–Zn–O1	177.25(11)
Zn–N2	2.114(2)	O1–Zn–N2	85.81(8)
Zn–O1N	2.226(2)	O1–Zn–N2	96.04(8)
		O1–Zn–O1N	83.18(8)
		O1–Zn–O1N	94.40(8)
		N2–Zn–O1N	104.46(9)
		N2–Zn–N2	95.64(12)
		N2–Zn–O1N	157.95(9)

and indicated that the complexes were thermally stable on the time scale of the experiment with very good reproducibility of their thermal behaviour. The DSC traces of $[ZnCl_2(L)]$ showed two endotherms, a large one at 46 °C (ΔH = 128 kJ mol^{-1}), corresponding to the melting point, followed by a smaller one at 143 °C (ΔH = 2 kJ mol^{-1}), assigned to the clearing process. For $[MnCl_2(L)]$, melting was observed at a slightly higher temperature (55 °C, ΔH = 94 kJ mol^{-1}), followed by a surprisingly high clearing point detected at 285 °C (ΔH = 2 kJ mol^{-1}). Thus, a great enhancement of the mesophase stability was achieved by simply changing the metal ion from Zn(II) to Mn(II). Nevertheless, $[ZnCl_2(L)]$ is of special interest as it is only the second example of a mesomorphic Zn(II) complex with simple, tetrahedral geometry. The first, reported by Giménez *et al.*, is based on co-ordination of $ZnCl_2$ to a pyrazole dimer,[22] while other, unsuccessful attempts have also been reported by Pucci *et al.* using 4,4′-bipyridine diesters.[23]

Small-angle powder X-ray diffraction allowed the unequivocal assignment of the mesophases. The experiments were carried out from the crystalline to the isotropic state with an X-ray pattern being recorded every 20 °C for each compound. The X-ray diffraction experiment data support the results obtained from optical microscopy and DSC for which a single mesophase was displayed by each of the complexes in the defined temperature ranges.

For $[ZnCl_2(L)]$, the X-ray pattern exhibited an intense, small-angle Bragg reflection, followed by a series of smaller reflections at mid-angles. In the wider angle region, a diffuse, broad-scattering was observed, centred around 4.5 to 4.6 Å, corresponding to the liquid-like order (short-range correlations) of the aliphatic chains and confirming the fluid-like nature of the mesophases (Fig. 5). Detailed viewing of the single reflection in the small-angle region reveals a shoulder that corresponds to an additional reflection; the proximity of both fundamental reflections explains the relative broadness of the base of the Bragg peak. These two reflections can be indexed as the 11 and 20 reflections of a rectangular lattice. The position of the other reflections allowed for an indexation compatible with such a rectangular symmetry. Moreover, since we do not observe the presence of any *hk* pairs with $h + k = 2n + 1$, the symmetry of the lattice can be further assigned as belonging to a *c2mm* plane group. The resulting calculated lattice parameters a and b, and columnar cross-section S are given in Table 3. X-Ray patterns recorded at other temperatures gave identical data. As a representative example, the diffraction pattern of the Col_r phase for $[ZnCl_2(L)]$ recorded at 100 °C is shown in Fig. 5.

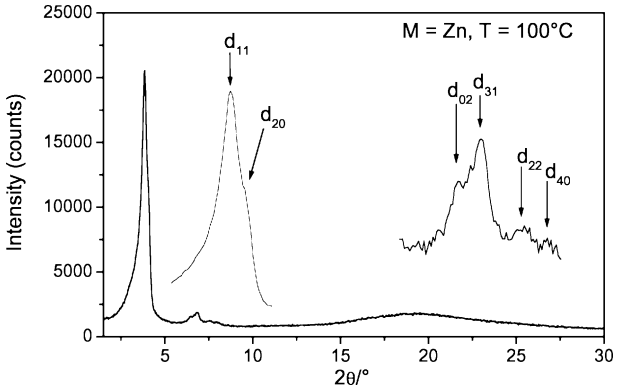

Fig. 5 X-Ray diffraction pattern of the Col_r of $[ZnCl_2(L)]$ {L = 2,6-diformyl-4-methylphenolbis[3′,4′,5′-tris(hexadecyloxy)phenylimine]} at 100 °C.

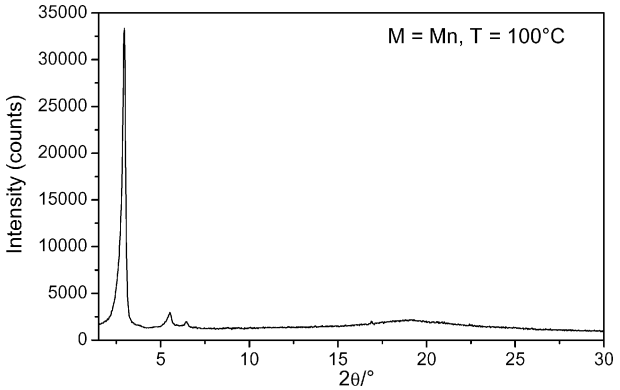

Fig. 6 X-Ray diffraction pattern of the Col_h of $[MnCl_2(L)]$ {L = 2,6-diformyl-4-methylphenolbis[3′,4′,5′-tris(hexadecyloxy)phenylimine]} at 100 °C.

For $[MnCl_2(L)]$, a series of three sharp reflections were observed in the small-angle region with reciprocal spacing ratio $1 : \sqrt{3} : \sqrt{4}$, characteristic of a two-dimensional hexagonal lattice and corresponding to the indexation $(hk) = (10)$, (11) and (20); additionally, a broad diffuse scattering was observed at 4.5 to 4.6 Å, confirming the liquid crystal nature of the mesophase (Fig. 6; Table 3). The X-ray pattern remained unchanged over the whole mesomorphic temperature range, with almost no variation within the intercolumnar distance. As a representative example, the diffraction pattern of the Col_h phase for $[MnCl_2(L)]$ recorded at 100 °C is shown in Fig. 6.

Table 3 Detailed indexation of the liquid-crystalline phases observed at 100 °C for the complexes $[ZnCl_2(L)]$ and $[MnCl_2(L)]$

M	d_{exp}/Å[a]	Intensity[b]	hk[c]	d_{theor}/Å[d]	Mesophase and parameters[e]
Zn	24.6	VS	11	24.6	Cr 46 [128] Col_r 143 [2] I
	23.3	VS	20	23.3	$Col_r - c2mm$
	14.35	S	02	14.5	a = 46.6 Å
	13.5	M	31	13.7	b = 29.0 Å
	12.2	M	22	12.3	S_{col} = 675.7 Å^2
	11.5	S	40	11.6	h = 4.7 Å
	4.6	br	h_{ch}		
Mn	25.45	VS	10	25.45	Cr 55 [94] Col_h 285 [2] I
	14.7	M	11	14.7	$Col_h - p6mm$
	12.7	M	20	12.7	a = 29.4 Å
	4.6	br	h_{ch}		S_{col} = 748.5 Å^2
					h = 4.25 Å

[a] d_{exp} and d_{theor} are the experimentally measured and theoretical diffraction spacings at 100 °C. [b] Intensity of the reflections: VS: very strong, S: strong, M: medium; br stands for broad (diffuse) reflections. [c] $[hk]$ are the indexation of the reflections, and h_{ch} are the short range periodicities determined by XRD corresponding to the liquid-like order of the molten chains. [d] d_{theor} and the lattice parameters a and b are deduced from the following mathematical expressions: for the Col_h, $\langle d_{10}\rangle = 1/N_{hk}[\Sigma_{hk} d_{hk}(h^2 + k^2 + hk)^{1/2}]$ where N_{hk} is the number of hk reflections and $a = 2\langle d_{10}\rangle/\sqrt{3}$, and for the Col_r, a and b are deduced from the following mathematical expressions: $a = 2d_{20}$, and $1/d_{hk} = \sqrt{(h^2/a^2 + k^2/b^2)}$. [e] Col_h: hexagonal columnar phase, Col_r: rectangular columnar phase, Cr: crystalline solid, I: isotropic liquid. S_{col} is the columnar cross-section area: $a^2\sqrt{3}/2$ (for Col_h) and $1/2ab$ (for Col_r). V_m is the molecular volume at 100 °C deduced from the equation in Fig. 8 (V_m = 3178.2 Å^3). h is the intracolumnar repeating distance, deduced directly from the measured molecular volume and the columnar cross-section according to $h = NV_m/S_{col}$, with N the number of complexes with this portion of column (hS_{col}).

In the Col_h phase, the cylindrical columns are organised onto a hexagonal lattice with the columns located at the nodes of a hexagonal cell (one column per cell) and the columnar axes perpendicular to this lattice plane (Fig. 7). The symmetry of the mesophase further requires that the molecules project a circular cross-section onto this lattice plane. In the case of the Col_r phase, however, the columns display an elliptical cross section and are disposed into a rectangular cell (two columns per lattice). Such elliptical cross-sections may be generated either by hindered molecular rotation of the non-discoid molecules around the columnar axis, or by the tilt of the molecular discs perpendicular to the columnar axis,[24] the ellipses being oriented along one main direction along the parameter a. The reasons for the formation of different mesophases upon changing the metal ion, and the greatly enhanced mesomorphic range for the Mn(II) complex, are not clear at this stage, the major difference between the two complexes being the smaller ionic radius for the Zn(II), some 10% lower than that for Mn(II).

The variation in the molecular volume of $[ZnCl_2(L)]$ was followed as a function of temperature (Fig. 8). On increasing the temperature, a discrete discontinuity in the molecular volume was found in the vicinity of the melting temperature, indicating a significant structural change due to the melting of the numerous aliphatic chains. Above the melting point, the

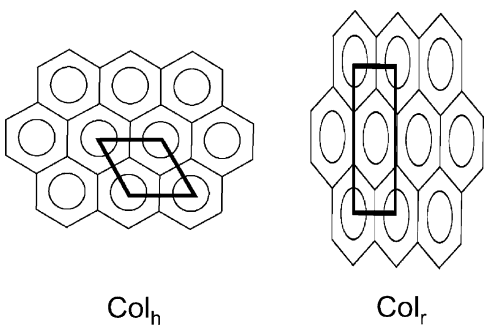

Fig. 7 Representation of the 2D lattice of the Col_h (left) and Col_r (right) mesophases formed by $[MnCl_2(L)]$ and $[ZnCl_2(L)]$, respectively.

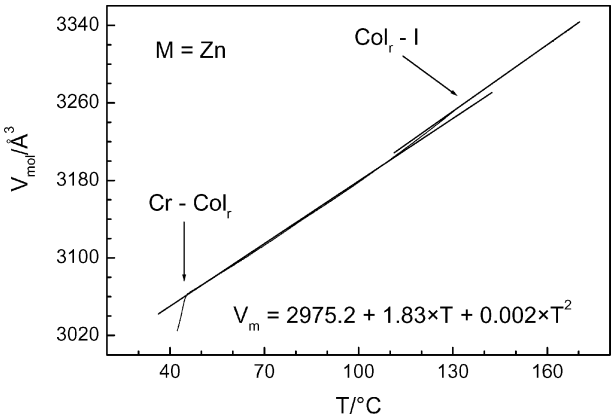

Fig. 8 Temperature-dependence of the molecular volume of $[Zn(L)Cl_2]$.

volume was found to vary almost linearly with T in the temperature range of the mesophase (the quadratic term being small compared to the linear term). The slope is in fairly good agreement with the volume variation in the methylene groups in liquid alkanes,[25] an indication that the effective volume of the aromatic part, V_{Ar},[26] is almost invariant with temperature in the mesophase. Indeed, the dilatation of the aromatic part can be considered negligible compared to that of the aliphatic chains which are in the molten state. Moreover, the transition to the isotropic liquid is evidenced by a small change in the molecular volume, and of the slope of the curve (V_m in isotropic liquid = 2956.5 + 2.27 T).

As is now well-described, columnar phases may be characterised by the columnar cross-section, S, and the stacking periodicity along the columnar axis, h.[27] Knowledge of these two structural parameters permits interpretation of the molecular packing inside the columns and a better understanding of the influence of this packing on the two-dimensional arrangement of the columns. The periodicity, h, the columnar cross-section, S_{col}, and the molecular volume, V_m, are linked analytically through the now well-established relationship:[27]

$$hS_{col} = NV_m \quad (1)$$

where N is the number of molecules within a volume fraction of column. Assuming that both complexes have about the same volume (in both case, the main contribution to the volume is the ligand) at the same temperature (*ca.* 3200 Å^3 at 100 °C), it is found that one complex (N = 1) occupies a slice of column on average 4.7 and 4.25 Å thick for $[ZnCl_2(L)]$ and $[MnCl_2(L)]$, respectively, in agreement with the observed XRD patterns. In order to propose a slightly more detailed model for the packing, it is necessary to take account of the overall shape of the complex as extrapolated from the single crystal structure. Thus, the complex can regarded as angular in nature defining an open V-shape, with the terminal chains at the two extremities of the V. Given the steric demands of these chains, it would then be expected that the next complex in the stack would fit approximately 'back-to-back' to minimise unfavourable interactions between these aliphatic areas. Thus, the complexes adopt an anti-parallel arrangement of the type postulated by Trzaska and Swager[28] and others[16a,29] in some structurally-related materials. Fortuitously, this arrangement

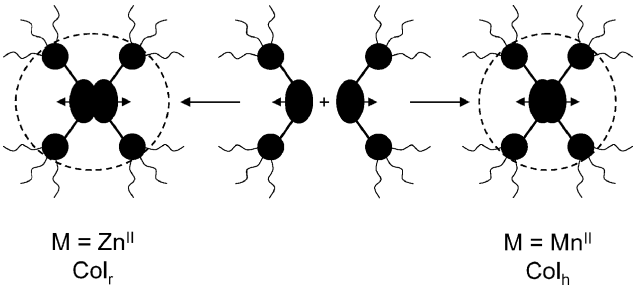

Fig. 9 Molecular arrangement forming columnar mesophases in time-averaged disc-like structures from the non-discoid metallomesogens.

also provides for an anti-parallel arrangement of the dipole arising from the $ZnCl_2$ fragment, which is also favourable energetically. In this way, each pair of molecules completes a discoid-like shell of chains surrounding the rigid part of the complex (Fig. 9).

In conclusion, we have confirmed that the M(II) complexes $[MCl_2(L)]$ {M = Mn, Zn; L = 2,6-diformyl-4-methylphenolbis[3′,4′,5′-tris(hexadecyloxy)phenylimine]} exhibit columnar mesophases, the nature and stability of which depend intimately upon the choice of metal ion. Thus, $[ZnCl_2(L)]$ exhibits a single mesophase with rectangular symmetry (Col_r) between 46 and 145 °C, whereas the Mn(II) analogue $[MnCl_2(L)]$ displays a purely hexagonal mesophase (Col_h) phase between 55 and 285 °C. Current work seeks to rationalise these observations *via* the study of related metallo–ligand systems and their analogues.

Experimental

Materials

All chemicals were purchased from commercial suppliers and were used without further purification. The EtOH used in the preparation of the anilines was dried over Mg turnings and freshly distilled prior to use. 2,6-Diformyl-4-methylphenol[17] and the 3,4,5-trialkoxyanilines[18] were prepared according to published methods.

Instrumentation

NMR spectra were recorded on a Bruker DPX300 FT-NMR spectrometer operating at 300.13 MHz for ^{1}H and 75.48 MHz for ^{13}C. Chemical shifts are referenced with respect to residual proton and carbon solvent (with δ_H = 7.26 ppm and δ_C = 77.0 ppm for $CDCl_3$). IR spectra were obtained on a Nicolet AVATAR 360 FT-IR spectrometer as KBr pellets. UV-Vis spectra were measured on a Philips PU 8720 spectrophotometer. FAB mass spectra were obtained on a Finnigan MAT TSQ-700 at the University of Wales, Swansea, with 3-nitrobenzyl alcohol (NOBA) as matrix. Elemental analyses (C, H, N) were carried out by the Analytical Department of the University of Nottingham. The transition temperatures and enthalpies were measured by differential scanning calorimetry with a Perkin-Elmer DSC-7 instrument operated at a scanning rate of 10 °C min^{-1} on heating. The apparatus was calibrated with indium (156.6 °C; 28.4 J g^{-1}) as the standard. For the dilatometry technique, the measurements were performed with

a high precision home-built apparatus, automatically computer-controlled, including data acquisition and temperature control within ±0.03 °C. The XRD patterns were obtained with two different experimental set-ups (I, II). In all cases, a linear monochromatic Cu-Kα_1 beam (λ = 1.5405 Å) was obtained using a sealed-tube generator (900 W) equipped with a bent quartz monochromator. In the first set, the transmission Guinier geometry (I) was used, whereas Debye–Scherrer-like geometry (II) was used in the second experimental set-up. In all cases, the crude powder was loaded into Lindemann capillaries of 1 mm diameter and 10 μm wall thickness. The initial set of diffraction patterns was recorded on an image plate; periodicities up to 80 Å can be measured, and the sample temperature controlled to within ±0.3 °C in the 20 to 350 °C temperature range. The second set of diffraction patterns (II) was recorded with a curved Inel CPS120 counter gas-filled detector linked to a data acquisition computer (periodicities up to 60 Å) or can be measured on image plates (periodicities up to 100 Å); the sample temperature controlled to within ±0.05 °C in the 20 to 200 °C temperature range. In each case, exposure times were varied from 1 to 24 h.

X-Ray crystallographic data

Data collection and processing. Single-crystal diffraction data were collected on a Bruker SMART1000 CCD area detector diffractometer,[30] equipped with an Oxford Cryosystem open-flow nitrogen cryostat,[31] using graphite-monochromated Mo-K$_\alpha$ radiation (λ = 0.71073 Å): 33)995 data collected ($2\theta_{max}$ = 58°, $-23 \le h \le 23$, $-19 \le k \le 18$, $-32 \le l \le 32$), 7432 unique data (R_{int} = 0.036) giving 5572 with $F > 2\sigma(F)$. Integrated intensities, corrected for Lorentz and polarisation effects, were obtained using the Bruker SAINT package,[32] as were the cell parameters. Multi-scan absorption corrections were applied, T_{min} and T_{max} of 0.876 and 1.000.

Structure solution and refinement. The crystal structure was solved by direct methods[33] and refined on F^2 using SHELXL-97.[34] All non-hydrogen atoms were refined with anisotropic displacement parameters except those of the MeOH and the partially occupied unbound nitrate. Additionally, the methanol was modelled as one fully occupied O atom with two half-occupied C sites and a second half-occupied MeOH group. Hydrogen atoms were placed in calculated positions and refined as part of a riding model except the methyl C(7) and hydrogen atoms on the phenol and the imine N(1)–hydrogen, which were located from ΔF syntheses. The N(1)–hydrogen was then refined with idealised geometry and included in a riding model and the C(7)–hydrogen atoms were refined as a rigid rotating group. The hydrogen atoms were not located for the solvate units but included in the formula for the unit cell contents and all quantities derived from them.

At final convergence $R[F \ge 4\sigma(F)]$ = 0.058, w$R[F^2$, all data] = 0.173, GoF = 1.02 for 386 parameters. The final difference Fourier synthesis showed a maximum peak of +1.07 and maximum trough of −0.61 eÅ^{-3}.

Synthetic procedures

Synthesis of 2,6-diformyl-4-methylphenolbis[3′,4′,5′-tris-(methoxy)phenylimine] (L′). A mixture of 2,6-diformyl-4-methylphenol (0.328 g, 2.00 mmol) and 3,4,5-tri(methoxy)aniline (0.732 g, 4.00 mmol) was heated at reflux in MeOH (150 cm^3) for 1 h, resulting in a red solution, which was left to evaporate at room temperature. The precipitate that formed after 24 h was collected by filtration and washed with a little cold MeOH, affording an orange-red crystalline solid in 89% yield (0.879 g). ^{1}H NMR (d_6-DMSO): δ_H 8.99 (2H, s, HC═N), 7.78 (2H, s, phenol-H$_{meta}$), 6.72 (4H, s, Ar-H), 3.83 (12H, s, m-OCH$_3$), 3.68 (6H, s, p-OCH$_3$), 2.35 (3H, s, phenol-CH$_3$). ^{13}C NMR (d_6-DMSO): δ_C 158.17 (HC═N), 153.32 (C$_q$), 145.08 (C$_q$), 136.44 (C$_q$), 133.35 (phenol-C$_{meta}$), 127.66 (C$_q$), 121.25 (C$_q$), 98.85 (Ar-CH), 60.08 (p-OCH$_3$), 55.94 (m-OCH$_3$), 19.85 (phenol-CH$_3$). IR (cm^{-1}): υ(C═N) 1626w and 1584s; υ(C–O) 1126. FAB-MS: m/z 494 ([M]$^+$). Anal. Calcd for $C_{27}H_{30}N_2O_7$: C, 65.57; H, 6.11; N, 5.66. Found: C, 65.40; H, 6.20; N, 5.57%.

Synthesis of 2,6-diformyl-4-methylphenolbis[3′,4′,5′-tris-(hexadecyloxy)phenylimine] (L). A mixture of 2,6-diformyl-4-methylphenol (0.0355 g, 0.216 mmol) and 3,4,5-tris(hexadecyloxy)aniline (0.352 g, 0.432 mmol) was heated at reflux in $CHCl_3$–MeOH (20 : 50 cm^3) for 2 h, resulting in a red solution, which was left to evaporate at room temperature. The precipitate which formed after 24 h was filtered off and washed with a little cold MeOH, affording an orange solid in 93% yield (0.260 g). ^{1}H NMR ($CDCl_3$): δ_H 8.80 (2H, br-s, HC═N), 7.26 (2H, s, phenol-H$_{meta}$), 6.51 (4H, s, Ar-H), 3.97 (12H, m, OCH$_2$), 2.37 (3H, s, phenol-CH$_3$), 1.88–1.26 (168H, m, CH$_2$), 0.88 (18H, 2 overlapping triplets, CH$_3$). ^{13}C NMR (d_6-DMSO): δ_C 158.17 (HC═N), 153.32 (C$_q$), 145.08 (C$_q$), 136.44 (C$_q$), 133.35 (phenol-C$_{meta}$), 127.66 (C$_q$), 121.25 (C$_q$), 98.85 (Ar-CH), 73.99, 73.60, 69.68, 69.28 (OCH$_2$), 31.94, 30.43, 29.77, 29.58, 29.51, 29.38, 29.14, 26.12, 22.69 (CH$_2$), 19.85 (phenol-CH$_3$). IR (KBr, cm^{-1}): υ(C–H) 2907vs and 2847vs; υ(C═N) 1626w and 1582m; υ(C–O) 1119s. FAB-MS: m/z 1756 ([M]$^+$). Anal. Calcd for $C_{117}H_{210}N_2O_7$: C, 79.98; H, 12.05; N, 1.59. Found: C, 80.03; H, 11.89, N, 1.54%.

Synthesis of dichloro-2,6-diformyl-4-methylphenolbis[3′,4′,5′-tris(methoxy)phenylimine]zinc(II) ([ZnCl$_2$(L′)]). A solution of 2,6-diformyl-4-methylphenol (0.0126 g, 0.0768 mmol) and 3,4,5-tri(methoxy)aniline (0.0282 g, 0.154 mmol) in $CHCl_3$ (20 cm^3) was stirred for 10 min, turning yellow, before adding a solution of $ZnCl_2$ (0.0105 g, 0.0770 mmol) in MeOH (7.5 cm^3). The orange precipitate which had formed upon addition of the metal salt dissolved once the solution was heated at reflux over 20 h. The resulting orange solution was left to stand and the orange needles which formed upon cooling were collected by filtration and washed with a little cold Et_2O, with a yield of 0.0412 g (85%). ^{1}H NMR (d_6-DMSO): δ_H 9.00 (2H, s, HC═N), 7.78 (2H, s, phenol-H$_{meta}$), 6.72 (4H, s, Ar-H), 3.83 (12H, s, m-OCH$_3$), 3.67 (6H, s, p-OCH$_3$), 2.35 (3H, s, phenol-CH$_3$). IR (cm^{-1}): υ(C═N) 1639m and 1595s; υ(C–O) 1128vs. FAB-MS: m/z 593 ([M − Cl]$^+$) and 630 ([M]$^+$). Anal. Calcd for $C_{27}Cl_2H_{30}N_2O_7Zn \cdot H_2O$: C, 49.98; H, 4.97; N, 4.32. Found: C, 50.28; H, 4.80; N, 4.26%. Orange columnar crystals of the complex were grown for single-crystal X-ray analysis by allowing the ligand in CH_2Cl_2 and $ZnCl_2$ in MeCN to diffuse and react together slowly over a number of weeks.

Synthesis of bis{2,6-diformyl-4-methylphenolbis[3′,4′,5′-tris-(methoxy)phenylimine]}nitratozinc(II) [Zn(L′)(NO$_3$)]NO$_3$. A solution of 2,6-diformyl-4-methylphenol (0.011 g, 0.067 mmol) and 3,4,5-tri(methoxy)aniline (0.0246 g, 0.134 mmol) in $CHCl_3$ (20 cm^3) was stirred for 10 min, turning yellow, before adding a solution of $Zn(NO_3)_2 \cdot 6H_2O$ (0.0199 g, 0.0669 mmol) in MeOH (7.5 cm^3). The resulting orange solution was heated at reflux for 20 h and then its volume was reduced to *ca.* 10 cm^3. The orange precipitate which had formed upon addition of the metal salt dissolved once the solution was heated at reflux over 20 h. Vapour diffusion of diethyl ether into this solution produced red cube-like crystals, suitable for study by X-ray diffraction, with a yield of 0.173 g (44%). ^{1}H NMR (d_6-DMSO): δ_H 8.99 (2H, s, HC=N), 7.78 (2H, s, phenol-H$_{meta}$), 6.72 (4H, s, Ar-H), 3.83 (12H, s, *m*-OCH$_3$), 3.68 (6H, s, *p*-OCH$_3$), 2.35 (3H, s, phenol-CH$_3$). ^{13}C NMR (d_6-DMSO): δ_C 158.17 (HC=N), 153.32 (C$_q$), 145.08 (C$_q$), 136.44 (C$_q$), 133.35 (phenol-C$_{meta}$), 127.66 (C$_q$), 121.25 (C$_q$), 98.85 (Ar-H), 60.08 (*p*-OCH$_3$), 55.94 (*m*-OCH$_3$), 19.85 (phenol-CH$_3$). IR (cm^{-1}): υ(C=N) 1638m and 1593s; υ(N–O) 1384vs; υ(C–O) 1128vs. FAB-MS: *m*/*z* 1118 ([M − NO$_3$]$^+$). Anal. Calcd for $C_{54}H_{60}N_6O_{20}Zn \cdot H_2O$: C, 54.21; H, 5.22; N, 7.02. Found: C, 53.80; H, 4.97; N, 6.74%.

Synthesis of dichloro-2,6-diformyl-4-methylphenolbis[3′,4′,5′-tris(hexadecyloxy)phenylimine]manganese(II) ([MnCl$_2$(L)]). A mixture of 2,6-diformyl-4-methylphenol (0.0131 g, 0.0798 mmol) and 3,4,5-tris(hexadecyloxy)aniline (0.130 g, 0.160 mmol) in $CHCl_3$ (20 cm^3) was stirred at room temperature for 10 min, turning to a yellow-orange solution. A solution of $MnCl_2 \cdot 4H_2O$ (0.0158 g, 0.0798 mmol) in EtOH (10 cm^3) was then added and the solution heated at reflux overnight. The resulting bright-orange solution was left to evaporate at room temperature and the precipitate that formed after 2 d was collected by filtration and washed with a small amount of cold EtOH, yielding 0.117 g (78%) of product as a bright-orange solid. IR (KBr, cm^{-1}): υ(C–H) 2919vs and 2850vs; υ(C=N) 1636m and 1589m; υ(C–O) 1117s. FAB-MS: *m*/*z* 1845 ([M − Cl]$^+$). Anal. Calcd for $C_{117}Cl_2H_{210}MnN_2O_7 \cdot H_2O$: C, 73.93; H, 11.24; N, 1.47. Found: C, 73.92; H, 11.23; N, 1.53%.

Synthesis of dichloro-2,6-diformyl-4-methylphenolbis[3′,4′,5′-tris(hexadecyloxy)phenylimine]zinc(II) ([ZnCl$_2$(L)]). A mixture of 2,6-diformyl-4-methylphenol (0.0142 g, 0.0865 mmol) and 3,4,5-tris(hexadecyloxy)aniline (0.141 g, 0.173 mmol) in $CHCl_3$ (40 cm^3) was stirred at room temperature for 10 min, turning to a yellow-orange solution. A solution of $ZnCl_2$ (0.0118 g, 0.0866 mmol) in EtOH (10 cm^3) was then added and the solution heated at reflux overnight. The resulting bright-red solution was left to evaporate at room temperature and the precipitate that formed after 1 d was collected by filtration and washed with a small amount of cold EtOH, yielding 0.156 g (95%) of product as a yellow-orange solid. ^{1}H NMR ($CDCl_3$): δ_H 9.38 (1H, br-s, HC=N), 8.16 (1H, s, HC=N), 7.67 (1H, s, phenol-H$_{meta}$), 7.22 (4H, s, phenol-H$_{meta}$), 6.95 (2H, s, Ar-H), 6.56 (2H, br-s, Ar-H), 4.08–3.89 (12H, m, OCH$_2$), 2.21 (3H, s, phenol-CH$_3$), 1.83–1.26 (168H, m, CH$_2$), 0.88 (18H, 2 overlapping triplets, CH$_3$). ^{13}C NMR ($CDCl_3$): δ_C 170.45 (C$_q$), 163.50 (HC=N), 158.18 (HC=N), 154.07 (C$_q$), 153.85 (C$_q$), 146.80 (phenol-C$_{meta}$), 142.68 (C$_q$), 141.04 (phenol-C$_{meta}$), 139.15 (C$_q$), 138.40 (C$_q$), 130.66 (C$_q$), 126.77 (C$_q$), 121.94 (C$_q$), 116.92 (C$_q$), 100.31 (Ar-CH), 97.93 (Ar-CH), 73.99, 73.60, 69.68, 69.28 (OCH$_2$), 31.94, 30.43, 29.77, 29.58, 29.51, 29.38, 29.14, 26.12, 22.69 (CH$_2$), 19.68 (phenol-CH$_3$), 14.09 (CH$_3$). IR (KBr, cm^{-1}): υ(C–H) 2919vs and 2850vs; υ(C=N) 1647m and 1592m; υ(C–O) 1119s. FAB-MS: *m*/*z* 1851 ([M − Cl]$^+$) and 1892 ([M]$^+$). Anal. Calcd for $C_{117}Cl_2H_{210}N_2O_7Zn \cdot H_2O$: C, 73.53; H, 11.18; N, 1.47. Found: C, 73.21; H, 11.12; N, 1.67%.

Acknowledgements

We thank the EPSRC and University of Nottingham for support and the EPSRC National Mass Spectrometry Service at the University of Wales, Swansea (UK) for mass spectra. MS gratefully acknowledges receipt of a Royal Society Wolfson Merit Award and of a Royal Society Leverhulme Trust Senior Research Fellowship. BD and DG greatly acknowledge the CNRS-ULP (UMR7504) for financial support, and Dr B. Heinrich for the dilatometry experiments and his constructive and helpful comments.

References

1 (*a*) N. Hoshino, *Coord. Chem. Rev.*, 1998, **174**, 77; (*b*) S. R. Collinson and D. W. Bruce, in *Transition metals in Supramolecular Chemistry*, ed. J. P. Sauvage, Wiley, New York, 1999, ch. 7, p. 285; (*c*) B. Donnio, D. Guillon, R. Deschenaux and D. W. Bruce, in *Comprehensive Coordination Chemistry II*, ed. J. A. McCleverty and T. J. Meyer, Elsevier, Oxford, 2004, vol. 7, p. 357; (*d*) *Metallomesogens: Synthesis Properties and Applications*, ed. J. L. Serrano, VCH, Weinheim, 1995.

2 (*a*) R. W. Date, E. Fernandez Iglesias, K. E. Rowe, J. M. Elliott and D. W. Bruce, *Dalton Trans.*, 2003, 1914; (*b*) M.-A. Guillevic, M. E. Light, S. J. Coles, T. Gelbrich, M. B. Hursthouse and D. W. Bruce, *J. Chem. Soc., Dalton Trans.*, 2000, 1437; (*c*) X.-H. Liu, M. N. Abser and D. W. Bruce, *J. Organomet. Chem.*, 1998, **551**, 271; (*d*) D. Lopez de Murillas, R. Pinol, M. B. Ros, J. L. Serrano, T. Sierra and M. R. de la Fuente, *J. Mater. Chem.*, 2004, **14**, 1117; (*e*) K. Binnemans, K. Lodewyckx, B. Donnio and D. Guillon, *Eur. J. Inorg. Chem.*, 2005, **8**, 1506; (*f*) K. Binnemans, Y. G. Galyametdinov, R. Van Deun, D. W. Bruce, S. R. Collinson, A. P. Polishchuk, I. Bikchantaev, W. Haase, A. V. Prosvirin, L. Tinchurina, I. Litvinov, A. Gubajdullin, A. Rakhmatullin, K. Uytterhoeven and L. Van Meervelt, *J. Am. Chem. Soc.*, 2000, **122**, 4335; (*g*) K. Binnemans, R. Van Deun, D. W. Bruce and Y. G. Galyametdinov, *Chem. Phys. Lett.*, 1999, **300**, 509; (*h*) S. R. Collinson, F. Martin, K. Binnemans, R. Van Deun and D. W. Bruce, *Mol. Cryst. Liq. Cryst.*, 2001, **364**, 745.

3 B. Donnio, *Curr. Opin. Colloid Interface Sci.*, 2002, **7**, 371.

4 (*a*) L. Douce, A. El-ghayoury, R. Ziessel and A. Skoulios, *Chem. Commun.*, 1999, 2033; (*b*) M. Ghedini and A. Crispini, *Comments Inorg. Chem.*, 1999, **21**, 53; (*c*) C. K. Lai, C.-H. Chang and C.-H. Tsai, *J. Mater. Chem.*, 1998, **8**, 599.

5 (*a*) L. Oriol and J. L. Serrano, *Angew. Chem., Int. Ed.*, 2005, **44**, 6618; (*b*) M. Cano, L. Oriol, M. Pinol and J. L. Serrano, *Chem. Mater.*, 1999, **11**, 94.

6 (*a*) Y. Yang, K. Driesen, P. Nockemann, K. Van Hecke, L. Van Meervelt and K. Binnemans, *Chem. Mater.*, 2006, **18**, 3698; (*b*) K. Binnemans, L. Malykhina, V. S. Mironov, W. Haase, K. Driesen, R. Van Deun, L. Fluyt, C. Gorller-Walrand and Y. G. Galyametdinov, *ChemPhysChem*, 2001, **2**, 680.

7 K. Binnemans and C. Gorller-Walrand, *Chem. Rev.*, 2002, **102**, 2303.

8 (*a*) T. Seshadri and H.-J. Haupt, Hans-Jurgen, *Chem. Commun.*, 1998, 735; (*b*) J. Malthête and J. Billard, *Mol. Cryst. Liq. Cryst.*, 1976, **34**, 117.

9 D. J. Saccomando, C. Black, G. W. V. Cave, D. P. Lydon and J. P. Rourke, *J. Organomet. Chem.*, 2000, **601**, 305.
10 R. Ziessel, *Coord. Chem. Rev.*, 2001, **216–217**, 195.
11 (*a*) D. E. Fenton and P. A. Vigato, *Chem. Soc. Rev.*, 1988, **17**, 69; (*b*) V. Alexander, *Chem. Rev.*, 1995, **95**, 273; (*c*) P. Guerriero, S. Tamburini and P. A. Vigato, *Coord. Chem. Rev.*, 1995, **139**, 17; (*d*) H. Okawa, H. Furutachi and D. E. Fenton, *Coord. Chem. Rev.*, 1998, **174**, 51; (*e*) M. Sakamoto, K. Manseki and H. Okawa, *Coord. Chem. Rev.*, 2001, **219–221**, 379; (*f*) P. Zanello, S. Tamburini, P. A. Vigato and G. A. Mazzocchin, *Coord. Chem. Rev.*, 1987, **77**, 165; (*g*) U. Casellato, P. A. Vigato and M. Vidali, *Coord. Chem. Rev.*, 1977, **23**, 31.
12 (*a*) C. J. O'Connor, D. Firmin, A. K. Pant, B. R. Babu and E. D. Stevens, *Inorg. Chem.*, 1986, **25**, 2300; (*b*) O. J. Gelling, A. Meetsma and B. L. Feringa, *Inorg. Chem.*, 1990, **29**, 2816; (*c*) S. Ryan, H. Adams, D. E. Fenton, M. Becker and S. Schindler, *Inorg. Chem.*, 1998, **37**, 2134; (*d*) O. Kahn, T. Malloh, J. Gouteron, S. Jeannin and Y. Jeannin, *J. Chem. Soc., Dalton Trans.*, 1989, 1117; (*e*) R. J. Majeste, C. L. Klein and E. D. Stevens, *Acta Crystallogr., Sect. C: Cryst. Struct. Commun.*, 1983, **39**, 52; (*f*) M. T. Rispens, O. J. Gelling, A. H. M. de Vries, A. Meetsma, F. van Bolhuis and B. L. Feringa, *Tetrahedron*, 1996, **52**, 3521; (*g*) M. Maekawa, S. Kitagawa, M. Munakata and H. Masuda, *Inorg. Chem.*, 1989, **28**, 1904; (*h*) C. J. Fahrni, A. Pfaltz, M. Neuburger and M. Zehnder, *Helv. Chim. Acta*, 1998, **81**, 507; (*i*) M. Mikuriya, Y. Hashimoto and S. Nakashima, *Chem. Commun.*, 1996, 295; (*j*) T. Mallah, M.-L. Boillot, O. Kahn, J. Gouteron, S. Jeannin and Y. Jeannin, *Inorg. Chem.*, 1986, **25**, 3058; (*k*) E. R. Quijano, E. D. Stevens and C. J. O'Connor, *Inorg. Chim. Acta*, 1990, **177**, 267, and references therein; (*l*) T. Koga, H. Furutachi, T. Nakamura, N. Fukita, M. Ohba, K. Takahashi and H. Okawa, *Inorg. Chem.*, 1998, **37**, 989; (*m*) H. Sakiyama, H. Tamaki, M. Kodera, N. Matsumoto and H. Okawa, *J. Chem. Soc., Dalton Trans.*, 1993, 591; (*n*) A. Asokan, B. Varghese and P. T. Manoharan, *Inorg. Chem.*, 1999, **38**, 4393; (*o*) W.-X. Zhang, C.-Q. Ma, X.-N. Wang, Z.-G. Yu, Q.-J. Lin and D.-H. Jiang, *Chin. J. Chem.*, 1995, **13**, 497; (*p*) J. Hermann and A. Erxleben, *Inorg. Chim. Acta*, 2000, **304**, 125; (*q*) M. Kwiatkowski, E. Kwiatkowski, A. Olechnowicz, D. M. Ho and E. Deutsch, *J. Chem. Soc., Dalton Trans.*, 1990, 3063; (*r*) P. Cheng, D. Liao, S. Yan, Z. Jiang, G. Wang, X. Yao and H. Wang, *Inorg. Chim. Acta*, 1996, **248**, 135.
13 (*a*) R. Robson, *Aust. J. Chem.*, 1970, **23**, 2217; (*b*) A. J. Atkins, A. J. Blake and M. Schröder, *J. Chem. Soc., Chem. Commun.*, 1993, 353; (*c*) A. J. Atkins, A. J. Blake and M. Schröder, *J. Chem. Soc., Chem. Commun.*, 1993, 1662; (*d*) A. J. Atkins, D. Black, A. J. Blake, A. Marin-Becerra, S. Parsons, L. Ruiz-Ramirez and M. Schröder, *Chem. Commun.*, 1996, 457; (*e*) D. Black, A. J. Blake, R. L. Finn, L. F. Lindoy, A. Nezhadali, G. Rougnaghi, P. A. Tasker and M. Schröder, *Chem. Commun.*, 2002, 340; (*f*) A. J. Atkins, D. Black, R. L. Finn, A. Marin-Becerra, A. J. Blake, L. Ruiz-Ramirez, W.-S . Li and M. Schröder, *Dalton Trans.*, 2003, 1730.
14 D. E. Fenton and H. Okawa, *Chem. Ber. Recl.*, 1997, **130**, 433, and references therein.
15 (*a*) M. Mikuriya, T. Fujii, S. Kamisawa, Y. Kawasaki, T. Tokii and H. Oshio, *Chem. Lett.*, 1990, 1181; (*b*) M. Mikuriya, T. Fujii, T. Tokii and A. Kawamori, *Bull. Chem. Soc. Jpn.*, 1993, **66**, 1675; (*c*) A. Erxleben and J. Hermann, *J. Chem. Soc., Dalton Trans.*, 2000, 569.
16 (*a*) F. Morale, R. W. Date, D. Guillon, D. W. Bruce, R. L. Finn, C. Wilson, A. J. Blake, M. Schröder and B. Donnio, *Chem.–Eur. J.*, 2003, **9**, 2484. See also: (*b*) S. T. Trzaska and T. M. Swager, *Chem. Mater.*, 1995, **7**, 2067; (*c*) C. K. Lai, A. G. Serrette and T. M. Swager, *J. Am. Chem. Soc.*, 1992, **114**, 7948; (*d*) A. G. Serrette, C. K. Lai and T. M. Swager, *Chem. Mater.*, 1994, **6**, 2252.
17 L. F. Lindoy, G. V. Meehan and N. Svenstrup, *Synthesis*, 1998, 1029.
18 A. Zinsou, M. Veber, H. Strzelecka, C. Jallabert and P. Fourré, *New J. Chem.*, 1993, **17**, 309.
19 D. Black, A. J. Blake, K. P. Dancey, A. Harrison, M. McPartlin, S. Parsons, P. A. Tasker, G. Whittaker and M. Schröder, *J. Chem. Soc., Dalton Trans.*, 1998, 3953.
20 (*a*) M. Prabhakar, P. S. Zacharias and S. K. Das, *Inorg. Chem.*, 2005, **44**, 2585; (*b*) N. Habbadi, M. Dartiguenave, L. Lamandé, M. Sanchez, M. Simard, A. L. Beauchamp and A. Souiri, *New J. Chem.*, 1998, **22**, 983.
21 H. Pizzala, M. Carles, W. E. E. Stone and A. Thevand, *J. Chem. Soc., Perkin Trans. 2*, 2000, 935.
22 R. Giménez, A. B. Manrique, S. Uriel, J. Barberá and J. L. Serrano, *Chem. Commun.*, 2004, 2064.
23 D. Pucci, G. Barberio, A. Crispini, O. Francescangeli, M. Ghedini and M. La Deda, *Eur. J. Inorg. Chem.*, 2003, 3649.
24 B. Donnio, B. Heinrich, H. Allouchi, J. Kain, S. Diele, D. Guillon and D. W. Bruce, *J. Am. Chem. Soc.*, 2004, **126**, 15258.
25 A. K. Doolittle, *J. Appl. Phys.*, 1951, **22**, 1471, volume of six aliphatic chains of 16 carbon atoms: $V_{ch} = 2550 + 1.94T$.
26 $V_{Ar} = 400 \pm 20$ Å^3.
27 D. Guillon, *Struct. Bonding*, 1999, **95**, 41.
28 S. T. Trzaska and T. M. Swager, *Chem. Mater.*, 1998, **10**, 438.
29 (*a*) C. K. Lai, Y. S. Pang and C. H. Tsai, *J. Mater. Chem.*, 1998, **8**, 2605; (*b*) C. D. Yang, Y. S. Pang and C. K. Lai, *Liq. Cryst.*, 2001, **28**, 191; (*c*) A. Bacchi, M. Carcelli, O. Francescangelli, F. Neve, P. Pelagatti and C. Pelizzi, *Inorg. Chem. Commun.*, 1999, **2**, 255; (*d*) H. D. Lin and C. K. Lai, *J. Chem. Soc., Dalton Trans.*, 2001, 2383.
30 Bruker, *SMART Area-Detector Software Package*, version 5.054, Bruker AXS, Inc., Madison, Wisconsin, USA, 1998.
31 J. Cosier and A. M. Glazer, *J. Appl. Crystallogr.*, 1986, **19**, 105.
32 Bruker, *SAINT frame integration software*, version 6.02a, Bruker AXS, Inc., Madison, Wisconsin, USA, 2000.
33 G. M. Sheldrick, *SHELXS-97, Program for solution of crystal structures*, University of Göttingen, Germany, 1997.
34 G. M. Sheldrick, *SHELXL-97, Program for refinement of crystal structures*, University of Göttingen, Germany, 1997.